

Normal Modes and Soliton Resonance for Vortices in 2D Classical Antiferromagnets

B. A. Ivanov*, A. K. Kolezhuk* and G. M. Wysin

Department of Physics, Kansas State University, Manhattan, KS 66506-2601

(August 8, 1995)

Magnon modes in the presence of solitons (vortices) in two-dimensional (2D) easy-plane antiferromagnets are studied. The vortex-magnon scattering matrix is obtained numerically. The analysis shows the presence of a new localized mode with a well-defined frequency determined by the strength of the anisotropy. It may be possible to observe this mode in resonance experiments for quasi-2D magnetic materials with a finite density of vortices.

PACS numbers: 75.10Hk, 75.30.Ds, 75.40Gb, 75.50Ee

It is well-known that strongly nonlinear topologically nontrivial excitations (solitons) play a special role in low-dimensional magnetic systems. For example, kinks in 1D systems are responsible for the destruction of long-range order at finite temperatures, and the presence of vortices in 2D systems gives rise to a special type of phase transition – the Berezinskii-Kosterlitz-Thouless transition [1]. Experimental observation of soliton signatures in the response functions is usually based on the fact that translational motion of solitons leads to the so-called soliton central peak, for review see [2–4]. Another possibility is to look for *internal* degrees of freedom of solitons, such as magnon modes *localized* on a soliton. Resonances at characteristic frequencies of an internal motion can be observed in electron spin resonance or inelastic neutron scattering (INS) experiments. In 1D such effects of “soliton magnetic resonance” were detected in the Ising-type antiferromagnet (AFM) CsCoCl₃ [5], and were predicted theoretically for Heisenberg AFMs [6]. In 3D, magnon modes localized on domain walls in AFMs were observed in thulium orthoferrite [7]. Presently, no experimentally testable examples of internal soliton dynamics in 2D are known. Moreover, only a *quasi-local* mode has been predicted for solitons in isotropic [8], XY-type [9], and easy-plane Heisenberg [10–12] 2D ferromagnets (FM).

The aim of the present Letter is to draw attention to the fact that in classical easy-plane Heisenberg 2D AFMs “out-of-plane” vortices have finite-frequency truly *localized* internal modes which may be detectable in resonance or INS experiments. We also numerically obtain the vortex-magnon S-matrix in the long-wavelength region, analyzing linearized perturbations of the vortex structure, for continuum and discrete lattice models.

The Model.— Consider the classical 2D-model of a Heisenberg easy-plane AFM, with the Hamiltonian

$$\hat{H} = J \sum_{\mathbf{n}, \mathbf{a}} \left[\vec{S}_{\mathbf{n}} \vec{S}_{\mathbf{n}+\mathbf{a}} + (\lambda - 1) S_{\mathbf{n}}^z S_{\mathbf{n}+\mathbf{a}}^z \right]. \quad (1)$$

Here $J > 0$ is the exchange constant, $0 < \lambda < 1$ describes anisotropy with the xy-plane as the easy-plane. Spins \vec{S}

are classical vectors on a 2D-square lattice with lattice constant a . \mathbf{n} denotes lattice sites of one sublattice, and \mathbf{a} 's are the set of displacements to the nearest-neighbors on the other sublattice. We are interested in the small anisotropy case $(1 - \lambda) \ll 1$.

A continuum model of AFM's can be derived from (1) in the usual way, see [2,4,6]. We define the magnetization vector $\vec{m} = (\vec{S}_{\mathbf{n}} + \vec{S}_{\mathbf{n}+\mathbf{a}})/2S$ and the sublattice magnetization vector $\vec{\ell} = (\vec{S}_{\mathbf{n}} - \vec{S}_{\mathbf{n}+\mathbf{a}})/2S$ on the set of nearest-neighbor pairs, with the constraints $\vec{m} \cdot \vec{\ell} = 0$, $\vec{m}^2 + \vec{\ell}^2 = 1$. Then, for low frequencies $\omega \ll 8JS/\hbar$ and small gradients, $|\nabla\ell| \ll 1/a$, the magnetization of an AFM is small, $|\vec{m}| \ll |\vec{\ell}| \simeq 1$. The magnetization can be considered as a “slave” variable, and can be expressed as $\vec{m} = \mathcal{X}(\vec{\ell} \times \partial\vec{\ell}/\partial t)$, where \mathcal{X} is a susceptibility defined below [Eq. (3)]. After eliminating \vec{m} one obtains equations for $\vec{\ell}$ only. Using the usual angular variables, ($\ell_x + i\ell_y = \sin\theta \exp(i\varphi)$, $\ell_z = \cos\theta$) these equations can be written in the form [4,6]

$$\begin{aligned} \nabla^2\theta + \sin\theta \cos\theta \left[\frac{1}{\Delta_o^2} - (\nabla\varphi)^2 + \frac{1}{c^2} \left(\frac{\partial\varphi}{\partial t} \right)^2 \right] &= \frac{1}{c^2} \frac{\partial^2\theta}{\partial t^2}, \\ \nabla \cdot (\sin^2\theta \nabla\varphi) &= \frac{1}{c^2} \frac{\partial}{\partial t} \left(\sin^2\theta \frac{\partial\varphi}{\partial t} \right) \end{aligned} \quad (2)$$

where c is the magnon phase velocity, Δ_o is the characteristic length scale. For the Hamiltonian (1)

$$\begin{aligned} \Delta_o &= (a/2)[\lambda/(1-\lambda)]^{1/2}, \quad c = 2(JS/\hbar a)(1+\lambda)^{1/2}, \\ \mathcal{X} &= (\hbar/16JS) [2(1+\lambda)]^{1/2}. \end{aligned} \quad (3)$$

Magnon and Vortex Excitations.— In the absence of vortices, this 2D-model has well-known magnon excitations about the classical AFM ground state. There are two branches of magnons: “in-plane” one with $\vec{\ell}$ oscillating in the easy-plane, and “out-of-plane” one with $\vec{\ell}$ oscillating in the z -direction, with out-of-plane and in-plane oscillations of \vec{m} , respectively. These have gapless and finite activation dispersion laws, respectively:

$$\omega_1(\vec{k}) = ck, \quad \omega_2(\vec{k}) = (\omega_o^2 + c^2k^2)^{1/2}, \quad \omega_o \equiv c/\Delta_o \quad (4)$$

where \vec{k} is the wave vector. These can be also obtained from a Taylor expansion of the dispersion law for the discrete model, see Ref. [13].

In the continuum models like Eq. (2), the out-of-plane vortex with the usual topological charges of vorticity ν and polarization p is described by the solution [14] $\theta = \theta_o(x)$, $x \equiv r/\Delta_o$, $\varphi = \varphi_o(\chi) = \nu\chi + \phi_o$, where (r, χ) are polar coordinates, $\theta_o(\infty) = \pi/2$, $\cos\theta_o(0) = (-1)^{p+1}$, and ϕ_o is a constant. Only the case $\nu = p = 1$ will be discussed here. The function $\theta_o(x)$ is described by an ordinary differential equation (ODE) which can be solved numerically by a shooting method, see [14,15].

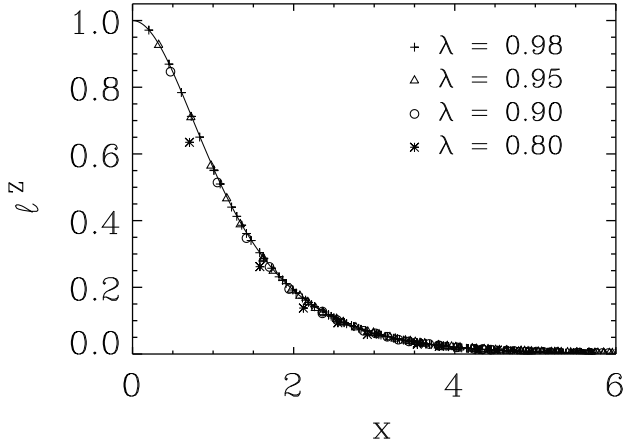


FIG. 1. The l_z vortex profile for $\nu = 1, p = 1$. Solid line — continuum solution for $\cos\theta_o$; points — l_z from discrete lattice model (1).

The distribution of spins in the static vortex also can be analyzed directly from the discrete model (1), see [10,11]. Energy minimization is carried out starting from a nearly in-plane structure, and redirecting spins along the effective fields due to the neighbors, iterating until convergence. The coincidence between the data of these approaches is surprisingly good, even for large anisotropy, see Fig. 1. Large discrepancies appear only for $\lambda < 0.8$ ($\Delta_o < a$), when the vortex structure is rapidly approaching the in-plane form.

Magnons on a vortex. Continuous approach.— Let's introduce small deviations of variables θ, φ from those in the vortex solution, $\theta = \theta_o(r) + \vartheta(r, \chi)$, $\varphi = \varphi_o + \mu(r, \chi)/\sin\theta_o(r)$. In local rotated coordinate frames, $\vec{e}_1, \vec{e}_2, \vec{e}_3$, where the axis \vec{e}_3 coincides with the \vec{l} -vector's direction in the unperturbed vortex, and

$$\begin{aligned} \vec{e}_1 &= \vec{e}_y \cos\varphi_o - \vec{e}_x \sin\varphi_o \\ \vec{e}_2 &= \vec{e}_z \sin\theta_o - \cos\theta_o(\vec{e}_x \cos\varphi_o + \vec{e}_y \sin\varphi_o), \end{aligned} \quad (5)$$

the variables ϑ, μ are the projections of the \vec{l} -vector on the local axes \vec{e}_1 and \vec{e}_2 : $\mu = \vec{l} \cdot \vec{e}_1$, $\vartheta = -\vec{l} \cdot \vec{e}_2$.

It is easy to get the coupled set of two partial differential equations for ϑ and μ :

$$\begin{aligned} [-\nabla_x^2 + U_1(x)] \vartheta + (2\nu \cos\theta_o/x^2) \partial\mu/\partial\chi &= (\omega^2/\omega_o^2) \vartheta, \\ [-\nabla_x^2 + U_2(x)] \mu - (2\nu \cos\theta_o/x^2) \partial\vartheta/\partial\chi &= (\omega^2/\omega_o^2) \mu, \end{aligned} \quad (6)$$

where $\nabla_x \equiv \Delta_o \nabla$, and the “potentials” are: $U_1(x) = (\nu^2/x^2 - 1) \cos 2\theta_o$, $U_2(x) = (\nu^2/x^2 - 1) \cos^2\theta_o - (d\theta_o/dx)^2$. Using the ansatz like that in [8],

$$\begin{aligned} \vartheta &= \sum_k \sum_{m=-\infty}^{+\infty} f_{k,m}(x) F_m(\chi) \exp(-i\omega t) + \text{c.c.}, \\ \mu &= \sum_k \sum_{m=-\infty}^{+\infty} g_{k,m}(x) G_m(\chi) \exp(-i\omega t) + \text{c.c.}, \end{aligned} \quad (7)$$

where $F_m(\chi) = a \exp(im\chi) + b \exp(-im\chi)$, $G_m(\chi) = i[a \exp(im\chi) - b \exp(-im\chi)]$, and a, b are arbitrary constants, one obtains a coupled set of ODEs for $f_{k,m}$ and $g_{k,m}$. Here $m = 0, \pm 1, \dots$; k and m are the full set of quantum numbers denoting the eigenvalues $\omega = \omega_{k,m}$. The presence of the combination of exponentials $\exp(\pm im\chi)$ with arbitrary coefficients is due to the degeneracy of the modes with $m = +|m|$ and $m = -|m|$. One can see that the coupling of ϑ and μ in Eq. (6) comes from the term with $\cos\theta_o(\partial/\partial\chi)$ only. This means that (i) the coupling vanishes exponentially at $x \gg 1$ ($r \gg \Delta_o$); (ii) there is no coupling for $m = 0$ modes, in contrast to the FM case [8,12].

Discrete Approach.— Numerical diagonalization for magnon modes on a vortex was performed for circular square lattice systems with radius $R < 20a$ and fixed boundary conditions, using the method of Ref. [11]. Spin deviations $S_{\vec{n}}^{\vec{x}}$ and $S_{\vec{n}}^{\vec{y}}$ from the static vortex spins were written in local coordinate frames for each spin in terms of creation/annihilation operators, e.g., $S_{\vec{n}}^{\vec{x}} = i\hbar \sum_{\alpha} [\mathbf{w}_{\vec{n},\alpha}^{(2)} B_{\alpha} - \mathbf{w}_{\vec{n},\alpha}^{(2)*} B_{\alpha}^{\dagger}]$, and replacing $\mathbf{w}_{\vec{n},\alpha}^{(2)} \rightarrow -\mathbf{w}_{\vec{n},\alpha}^{(2)}$ to give $S_{\vec{n}}^{\vec{y}}$. Here $\alpha = \{k, m\}$. The matrix equations of motion for the $\{\mathbf{w}_{\vec{n},\alpha}^{(1)}, \mathbf{w}_{\vec{n},\alpha}^{(2)}\}$ coefficients was diagonalized numerically. Some modes for a system of radius $R = 8a$ with a vortex at the center are shown in Fig. 2; the \mathbf{w} 's are represented as arrows in the complex plane.

Using the semiclassical condition, $B_{\alpha} \sim \exp(-i\omega_{\alpha} t)$, connections between the $\{\mathbf{w}_{\vec{n},\alpha}^{(1)}, \mathbf{w}_{\vec{n},\alpha}^{(2)}\}$ coefficients and $\{f_m, g_m\}$ can be established. Using the formula $\vec{e}_{\vec{x},\vec{y},\vec{z}} = \vec{e}_{1,2,3}$ for the first $\vec{e}_{\vec{x},\vec{z}} = -\vec{e}_{1,3}$, $\vec{e}_{\vec{y}} = \vec{e}_2$ for the second one, with \vec{e}_i determined by (5), we have

$$2S\vec{l}_{\vec{n}} = (S_{\vec{n}}^{\vec{x}} + S_{\vec{n}+\mathbf{a}}^{\vec{x}}) \vec{e}_1 + (S_{\vec{n}}^{\vec{y}} - S_{\vec{n}+\mathbf{a}}^{\vec{y}}) \vec{e}_2, \quad (8)$$

and a similar equation for $2S\vec{m}_{\vec{n}}$, changing the signs before $S_{\vec{n}+\mathbf{a}}^{\vec{x},\vec{y}}$. Then one can show that the connections are:

$$\begin{aligned} \mathbf{w}_{\vec{n},\alpha}^{(1)} - \mathbf{w}_{\vec{n}+\mathbf{a},\alpha}^{(1)} &= -if_{\alpha}(r) F_m(\chi), \\ \mathbf{w}_{\vec{n},\alpha}^{(1)} + \mathbf{w}_{\vec{n}+\mathbf{a},\alpha}^{(1)} &= -\omega \mathcal{X} g_{\alpha}(r) G_m(\chi), \end{aligned} \quad (9)$$

and similarly for $\mathbf{w}_{\vec{n},\alpha}^{(2)}$, changing $if \rightarrow \omega \mathcal{X} f$ and $i\omega \mathcal{X} g \rightarrow g$. The equations (9) work well for low-energy modes.

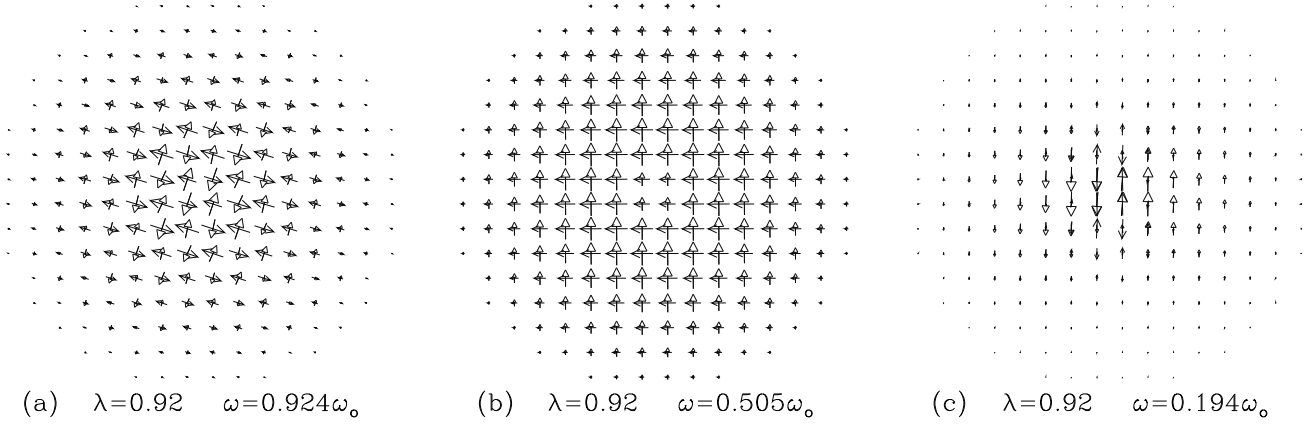


FIG. 2. Modes from numerical diagonalization. Complex amplitudes $w_{\mathbf{n},\alpha}^{(1)}$ and $w_{\mathbf{n},\alpha}^{(2)}$ are shown as open arrows (\rightarrow) and closed arrows (\rightarrow), respectively. (a) Local mode, with $w_{\mathbf{n},\alpha}^{(2)}$ arrows enlarged by a factor of 4. (b) Nonlocal $m = 0$ mode, with $w_{\mathbf{n},\alpha}^{(1)}$ arrows enlarged by a factor of 8. (c) $m = \pm 1$ translational mode, with equal scales for $w_{\mathbf{n},\alpha}^{(1)}$ and $w_{\mathbf{n},\alpha}^{(2)}$ arrows.

For example, the arrows for $w_{\mathbf{n},\alpha}^{(1)}$ in Fig. 2a, b, are perpendicular to those for $w_{\mathbf{n},\alpha}^{(2)}$; in different sublattices they are antiparallel for the mode with $g \approx 0$ (Fig. 2a), and parallel for the $f \approx 0$ mode (Fig. 2b). For the case $m \neq 0$ (e.g., Fig. 2c), the ratio a/b [Eq. (7)] can take the values ± 1 , and degenerate pairs of modes ($\pm m$) combine to form linear combinations with structure $(w_{\mathbf{n},\alpha}^{(1)}, w_{\mathbf{n},\alpha}^{(2)}) \propto (\cos m\chi, \sin m\chi)$.

Local mode.— For $m = 0$, the equations for f and g are uncoupled and have the forms of usual Schrödinger equations (SE). Then it is easy to show that the equation for $g_{k,0}(x)$ has a gapless continuous spectrum only, with the usual oscillating asymptotic scattering form far from the vortex,

$$r^{-1/2} \cos(kr + \phi), \quad k = |\omega|/c. \quad (10)$$

The equation for $f_{k,0}$ can be put in the form of a SE with the potential $U_1(x)$, where $U_1(x) \simeq -1 + 1/x^2$ at $x \rightarrow 0$ and $U_1(x) \simeq 1 - 1/x^2$ at $x \gg 1$. So, the continuous spectrum of this problem has a gap, and for $\omega^2 > \omega_o^2$ can be put in form (10) far from the vortex, with $kc = (\omega^2 - \omega_o^2)^{1/2}$. But the presence of the attractive part of the potential, $U_1(x) < U_1(\infty) = 1$, gives the possibility of the appearance of a local mode with the frequency ω_ℓ , $\omega_\ell^2 < \omega_o^2$, with well-pronounced exponential decay, $f_{\ell,0} \propto \exp[-x(1 - \omega_\ell^2/\omega_o^2)^{1/2}]$. The analysis of this mode was done numerically by using a shooting method [15] in finite circular systems of radius $R = X\Delta_o$, with the conditions, $f(0) = f(X) = 0$, $X \leq 40$. Comparison with the results of exact diagonalization have shown very good agreement of the two approaches, see Fig. 3. The dependence of ω_ℓ on R is very weak for large enough R , e.g., $\omega_\ell \simeq 0.958\omega_o$ for $R \simeq 9\Delta_o$, and $\omega_\ell \simeq 0.955\omega_o$ for $R \simeq 40\Delta_o$. Size effects become strong only for $R < (1 - \omega_\ell^2/\omega_o^2)^{-1/2}\Delta_o \simeq 3.4\Delta_o$. The presence of a literally

local mode inside the continuous spectrum is a unique property of AFM-vortices. It should manifest itself in response functions of the AFM's with vortices, and since the excitation of the local mode requires no momentum transfer, such resonance can in principle be observed in ESR experiments.

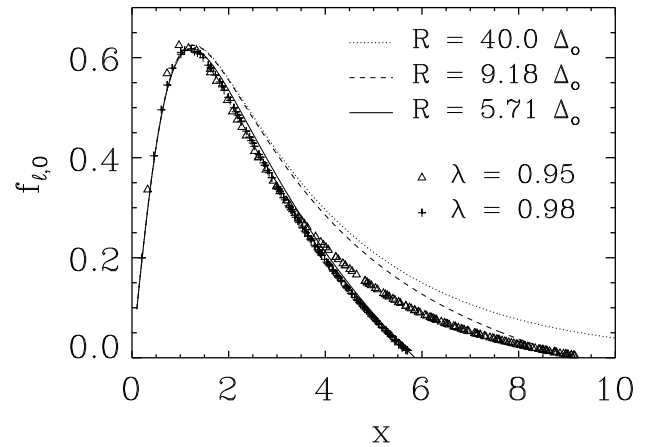


FIG. 3. The local mode, $f_{\ell,0}$, from continuum theory (lines) and from discrete model numerical diagonalization (symbols) for radius $R = 20a$ circular systems.

Vortex-Magnon S-matrix.— For $m \neq 0$ modes the in- and out-of-plane $\vec{\ell}$ oscillations are coupled strongly near the vortex center. For $x \ll 1$ ($r \ll \Delta_o$) one has the Taylor expansions

$$f_m \pm mg_m = C_{(\pm)} x^{|\nu \pm m|} (1 + a_1^{(\pm)} x^2 + a_2^{(\pm)} x^4 + \dots),$$

where the coefficients $a_n^{(\pm)}$ are determined by ω^2 and arbitrary parameters $C_{(\pm)}$. The presence of non-scale coef-

efficient $\varepsilon \equiv C_{(-)}/C_{(+)}$ is a special property of the eigenvalue problem (6); the ratio of amplitudes of in- and out-of-plane oscillations in the wave with given frequency ω is regulated by ε .

Far from the vortex core, $x \gg 1$, the coupling term in (6) is exponentially small, $\cos\theta_o \propto \exp(-x)$. For $r \gg \max(\Delta_o, 1/k)$ the solution for g can be expressed in the oscillating form (10). For $f_{k,m}(r)$ one has asymptotics with linear combinations of exponents like $r^{-1/2}A_{(\pm)}\exp(\pm\kappa r)$, where $\kappa = c^{-1}(\omega_o^2 - \omega^2)^{1/2}$, and constants A_{\pm} depend on ω and $C_{(\pm)}$. For $\omega^2 > \omega_o^2$ only oscillating asymptotics like (10) appear.

In the most interesting region of small frequencies, $\omega^2 < \omega_o^2$, the eigenfunction with oscillations of $g_{k,m}(x)$ combined with exponentially decaying $f_{k,m}(x)$ can be constructed using the shooting method, “killing” the growing exponent in $f_{k,m}(x)$ by choosing an appropriate value of ε . Numerically, the boundary condition $f(X) = 0$ was applied, and very well-pronounced exponential decay of $f(x)$ resulted, even for $X \simeq 40$. The scattering problem can be analyzed from these calculations. In order to explain let’s consider the magnons without a vortex. The solutions can be represented in the form (7) with $f_{k,m} = 0$, $g_{k,m} = J_m(kr)$, which is (10) with a defined value of the phase $\phi = -(\pi/4)(2m+1)$. In the presence of the vortex ϕ takes another value, which means the asymptotic is in the form $g_{k,m} \propto J_m(kr) + \rho_m(k)Y_m(kr)$, where Y_m is a Neumann function. Obviously, the coefficient ρ_m is the measure of the intensity of scattering, see Fig 4. Then, the S-matrix can be obtained from $S_m(k) = (1 - i\rho)/(1 + i\rho)$. The values of $\rho_m(k)$ are smaller for larger values of m , for example, $\rho_m(k) \leq 10^{-2}$, 2×10^{-3} and 2×10^{-5} for $m=3,4$ and 6.

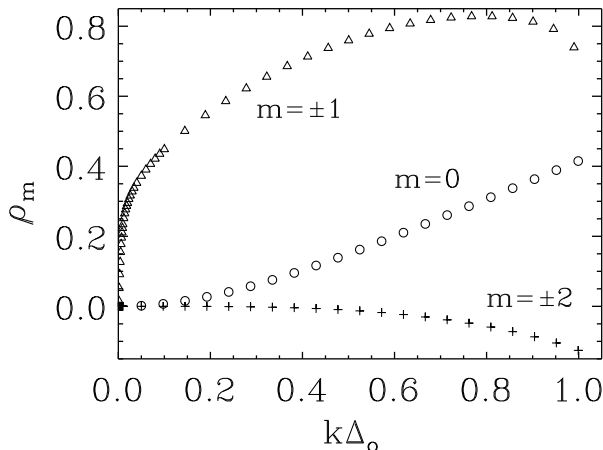


FIG. 4. The $\rho_m(k)$ dependence for $m = 0, \pm 1$ and ± 2 , extracted from the shooting solutions.

It is well known that the presence of a quasi-local mode with large lifetime at $\omega \simeq \omega_{ql}$ gives a sharp maximum in

$S_m(k_{ql})$, $k_{ql} = \omega_{ql}/c$. The components of the S-matrix for all m 's excluding $m = \pm 1$ have no such maxima at $k\Delta_o \neq 0, 1$, and the maximum for $m = \pm 1$ is very wide. It means that there is no chance to have a well-defined quasi-local mode at $\omega_\ell \neq 0, \omega_o$ for $|m| \neq 1$. However, at $k \rightarrow 0$, the $\rho_1(k)$ dependence is very fast, possibly indicating a root type singularity. The eigenfunctions near this point have a special shape with a well-defined maximum at $r \leq \Delta_o$, which is fitted by the translational mode functions ($f_o = (d\theta_o/dx)$, $g_o = (1/x)\sin\theta_o$), and a small amplitude oscillating tail. It means that the quasi-local mode with $m = \pm 1$, $\omega \simeq 0$ is present, as in FMs.

Acknowledgements.— We gratefully acknowledge the support of a NRC/NAS COBASE Grant and NSF Grant DMR-9412300. B.I. and A.K. were partially supported by UCST Grant 2.3/194 and ISF Grant UB7200.

* Permanent Address: Institute of Magnetism, Ukrainian Academy of Sciences, 252142 Kiev.

- [1] V. Berezinskii, Sov. Phys. JETP **32**, 493 (1970); J. M. Kosterlitz and D. J. Thouless, J. Phys. C **6**, 1181 (1973).
- [2] H.-J. Mikeska and M. Steiner, Adv. Phys. **40**, 191 (1991).
- [3] D. G. Wiesler, H. Zabel, and S. M. Shapiro, Z. Phys. B **93**, 227 (1994).
- [4] B. A. Ivanov and A. K. Kolezhuk, Low Temp. Phys. **21**, 355 (1995).
- [5] J.-P. Boucher, G. Rius, and Y. Henry, Europhys. Lett. **4**, 1073 (1987).
- [6] B. A. Ivanov and A. K. Kolezhuk, Phys. Rev. Lett. **74**, 1859 (1995).
- [7] G. A. Kraftmakher, V. V. Meriakri, A. Ya. Chervonenkis, and V. I. Shcheglov, Sov. Phys. JETP **36**, 714 (1973).
- [8] B. A. Ivanov, JETP Lett., **61**, N11 (1995).
- [9] B. V. Costa, M. E. Gouvêa and A. S. T. Pires, Phys. Lett. A **165**, 179 (1992); A. Pereira, A. S. T. Pires, and M. E. Gouvêa, Sol. St. Comm. **86**, 187 (1993).
- [10] G. M. Wysin, Phys. Rev. B **49**, 8780 (1994).
- [11] G. M. Wysin and A. R. Völkel, Phys. Rev. B — *in press*.
- [12] B. A. Ivanov, F. G. Mertens, H.-J. Schnitzer and G. M. Wysin, to be published.
- [13] A. R. Völkel, G. M. Wysin, A. R. Bishop and F. G. Mertens, Phys. Rev. B **44**, 10,066 (1991).
- [14] A. M. Kosevich, V. A. Voronov and I. V. Manzhos, Sov. Phys. JETP, **57**, 86 (1983).
- [15] W. H. Press *et al.*, *Numerical Recipes*, Cambridge University Press (1986).